*Arabian Journal of Chemical and Environmental Research*

*Vol. 08 Issue 2 (2021) 315–335*

# Removal of Pendimethalin from Aqueous Solution by Carbon prepared from Bambara Groundnut (*vigna subteranean*) Shells

**T. A. Nyijime[1]* A. M Ayuba[1] and H. F Chahul[2]**

[1]*Research Laboratory, Department of Chemistry, Faculty of Science. Bayero University, P.M.B.3011 Kano, Nigeria.*

[2]*Research Laboratory, Department of Chemistry, Faculty of Science, Federal University of Agriculture P.M.B. 2373, Makurdi, Nigeria.*

*Received 01 July 2021, Revised 02 Sept 2021, Accepted 04 Sept 2021*

**Abstract**

Batch removal of Pendimethalin (PE) from aqueous solution using carbonized bambara groundnut shells (CBGNS) adsorbent under different experimental conditions was investigated in this study. The CBGNS were characterized by pore volume, bulk density, moisture content, FT-IR spectroscopy and SEM spectroscopy analysis. The influences of initial PE molecule concentration (10 to 60 $mg \cdot l^{-1}$), pH (3 to 8), contact time (20 to 120 mins) and adsorbent dosage (0.2 to 1.2g) have been reported. Adsorption of PE is highly pH-dependent and the result indicate that the optimum pH for the removal was found to be 6 for CBGNS. Adsorption equilibrium data were fitted to Langmuir, Freundlich, Temkin and Dubinin-Radushkevich isotherm models and the equilibrium data for CBGNS were best represented by the Freundlich isotherm. A comparison of kinetic models applied to the adsorption of PE molecule on the CBGNS was evaluated for the pseudo first-order, the pseudo second-order, Elovich and intraparticle diffusion kinetic models, respectively. Results show that the pseudo second-order kinetic model was found to correlate the experimental data well. Thermodynamic parameters such as enthalpy (ΔH), entropy (ΔS) and free energy (ΔG) were evaluated.

***Keywords*:** Adsorption; Pendimethalin; Adsorption kinetics; Carbonized adsorbent; Aqueous solution

*Corresponding author.

*E-mail address:* thomasnyijime@gmail.com

## 1. Introduction

The wide spread use of pesticides in agriculture, and domestic activities for controlling pests kept raising and polluting water bodies day by day [1]. Due to the threat posed by such act to the

ISSN : 2458-6544 

ecosystem, therefore, there is need to curb such practices [2]. Pesticides form a strong class of water pollutants, as they are mostly non-biodegradable [3]

Pendimethalin *(*3, 4-dimethyl-2, 6-dinitro-N-pentan-3-ylaniline) is a selective dinitroaniline herbicide which acts as a microtubule disruptor by inhibiting cell division and cell elongation in plants. It is almost non-volatile and its half-life in soil condition is about 30- 90 days but varies depending on various environmental factors like pH, moisture content, temperature and microbial activity [4]. Pendimethalin is a selective herbicide, applied before emergence to cereals, maize, and rice, and with shallow soil incorporation before seeding bean, cotton, soy beans, and groundnuts. In vegetable crops, it is applied before emergence or transplanting, and it is also used to control suckers on tobacco [4].

The wide use of pendimethalin however, negatively impacts the water quality and poses threat to the environment and ecosystem, even though its use is in a limited amount despite its use is within the permitted dosage. Adsorption technique is favourable for pendimethalin removal due to its simplicity as well as the availability of a wide range of adsorbents. The use of the activated carbon in removing many pesticides from aqueous solution has been demonstrated in the literature [2, 5]. However due to the high cost of activated carbon, its usage in the removal of pendimethalin is less attractive. Thus, there is a demand for alternative adsorbents which are made of in expensive materials such as agricultural wastes. Since, BGNS is abundant in Nigeria and constitute a waste disposal problem. This material can be easily processed as a good adsorbent. Most of the reported work on the use of Bambara groundnut shells product is on the removal of dyes and has to do with the ability of these adsorbent in adsorbing the dyes. There are few reports on the specific mode of action of the adsorbent and the extent of adsorption: [5, 6, 7, 8].

The aim of the present study is to remove pendimethalin herbicide from aqueous solution using carbonized bambara groundnut shells. More also evaluate the equilibrium adsorption data using the notable adsorption isotherms, kinetics and thermodynamics studies as well as proposing the possible adsorption mechanism from the insight obtained from adsorption isotherms studies. The molecular structure of pendimethalin herbicide is shown thus;

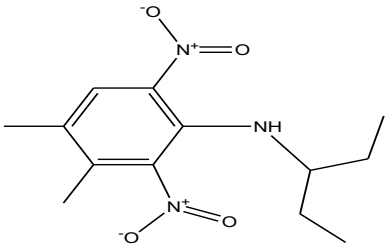


**Fig. 1**. Molecular structure of Pendimethalin (3, 4-dimethyl-2, 6-dinitro-N-pentan-3-ylaniline)

## 2. Materials and methods

### 2.1. Plant material

Bambara groundnut shell (*Vigna subterranean*) (BGNS) were obtained from farm in Zaki-Biam, Ukum Local Government area of Benue State, Nigeria. Bambara groundnut is *Voandzeia subterranean* (L) *thouars*, synonyms of *Vigna subterranea* and belongs to plantea of the family of *Fabaceae* and sub family of *Faboidea*. An annual herb with short creeping much branched stems, rooting at node. The pods are hard and wrinkled when dry. Each pod contains one or two seeds. The colour of the seed varies from black, brown or red and may be mottled with various colures [9]. Before consumption, the hulls are removed and generally regarded as waste.

### 2.2. Preparation of Adsorbent

The Bambara groundnut shells obtained, after removing the seeds from the pods, were thoroughly washed with water to remove dust and other impurities. The shells were then air-dried and oven-dried at 80 $^0$C to constant weight in the laboratory. The dried shells were then pulverized and sieved into fine particles as previously described by Akinola *et al.* [10]. 100g of Bambara ground nut shell (BGNS) was carbonized in the muffle furnace at 450 $^0$C for 1 hour. The carbon produced was washed with plenty of water and dried as described by Ash *et al.* [11] and was kept for further usage.

### 2.3. Preparation of Pendimethalin (PE) solution

1000mg/l of the PE solution was prepared by mixing 2ml of the 500mg/l pendimethalin solution in 1000ml standard volumetric flask and made up to mark. Serial dilution was carried out using distilled water to give solution concentration of 10, 20, 30, 40, 50 and 60mg/l of pendimethalin solution.

### 2.4. Determination of bulk density

The bulk density of carbonized Bambara groundnut shells (CBGNS) was determined using Archimedes's principle by weighing 10cm$^3$ measuring cylinder before and after filling with the samples. The measuring cylinder was then dried and the sample was packed inside the measuring cylinder, leveled and weighed. The weight of the sample packed in the measuring cylinder was determined from the difference in weight of the filled and empty measuring cylinder. The volume of water in the container was determined by taking the difference in weight of the empty and water filled measuring cylinder. The bulk density was determined using the equation (1) [12].

$$\text{Bulk density} = \frac{W_2 - W_1}{V} \quad (1)$$

$W_1$ is weight of empty measuring cylinder, $W_2$ is Weight of cylinder filled with sample and V is Volume.

### 2.5. Determination of Moisture Content

This was done by the gravimetric method as described by AOAC, [13] and Onwuka, [14]. 5g of CBGNS was weighed and put into a weighed crucible. The crucible and its sample content were dried in the oven at 105 $^{o}$C for 3 hours in the first instance. It was cooled in desiccator and reweighed. The weight was recorded while the sample was returned to the oven for further drying. Sample was heated for the second time at 105 °C for 30 min, cooled in desiccator and weighed again. The procedure was repeated several times at the same temperature for 15 min until a constant weight was obtained. The percentage moisture content of each sample was calculated using equation (2):

$$\% \text{ moisture content} = \frac{W_2 - W_3}{W_2 - W_1} \text{ X } 100 \quad (2)$$

Were; $W_1$ is Weight of crucible, $W_2$ is Initial weight of crucible with sample, $W_3$ is Final weight of crucible with sample

### 2.6. Determination of Pore (Void) Volume

In order to determine the pore volume of the CBGNS, 2.0 g of the sample was immersed in water and boiled for 15 min. After the air in the pores had been displaced, the sample was superficially dried and reweighed. The increase in weight divided by the density of water gave the pore volume [5].

### 2.7. Scanning Electron Microscope (SEM)

The surface morphological change of CBGNS samples were investigated using Scanning Electron Microscope (Phenom World Eindhoven) Scanned micrographs of CBGNS before and after adsorption were taken at an accelerating voltage of 15.00 kV and x500 magnification.)

### 2.8. Fourier transforms infrared (FT-IR) analysis

FTIR analysis of CBGNS before and after adsorption was carried out using Cary 630 Fourier Transform Infrared Spectrophotometer Agilent Technology. The resulting residue collected was dried for FTIR analysis. The analysis was done by scanning the sample through a wave number range of 650 – 4000 $cm^{-1}$; 32 scans at 8$cm^{-1}$resolution.

### 2.9. Batch Adsorption Experiment

The equilibrium adsorption of the pendimethalin (PE) molecule onto CBGNS was carried out by contacting 0.2g of the substrate with 10$cm^3$ of different concentrations from 10 mg/L – 60mg/L in 250cm3 Pyrex conical flasks intermittently for 2h on the incubator shaker (Innova 4000 Medol). The mixture was filtered and the residual concentration of the filtrate was analyzed using UV-visible

Spectrophotometer (Perkin-Elemer). The same method was used while varying the contact time, the adsorbent dosage, and temperature of adsorption during optimization experiments.. The amount of adsorbed (mg/g) was calculated using the formulae mass balance of the equation (3) [5].

$$\text{Pendimethalin uptake, } q_e = \frac{(Co-Ce)V}{m} \quad (3)$$

Where: $C_o$ and $C_e$ are the initial and equilibrium concentration (mg/l) respectively of pendimethalin solution, V is the volume of pendimethalin in solution (L), and m is the mass (g) of the adsorbent.

The percentage of removed pendimethalin concentrations ($R_{em}$ %) in solution was calculated using equation (4) [16].

$$\% \text{ Pendimethalin Removal} = \frac{Co-Ce)}{Co} \times 100 \quad (4)$$

The data was fitted into the following isotherms: Langmuir, Freundlich, Temkin and Dubinin-Raduskevich isotherms.

### 2.9.1 Optimization of adsorption parameters

#### i. Effect of pH

In order to determine adsorption density of the effect of pH onto CBGNS. The experiments were performed in the pH range of 3 to 8 while keeping all other parameters constant PE concentration 50mg/L; adsorbent dose 0.1g; contact time 24h; temperature 25◦C). The solution pH was adjusted to the required value using 0.1MHCl or NaOH, and pH was measured using a pH meter (MP220). The filtrates obtained from mixture were analyzed for residual un- adsorbed PE using UV visible spectrophotometer. The quantity adsorbed was calculated from the equation (3) [17].

#### ii. Effect of contact time

0.1 g carbonized Bambara groundnut shells were weighed separately into a 100ml conical flasks. A 10$cm^3$ of the optimum concentration (60 mg/L PE) solution was added into the beaker. Each solution was agitated for different time intervals of 20, 40, 60, 80, 100 and 120 minutes to investigate the effect of contact time. After the completion of the reaction, the mixtures were filtered, followed by the determination of the residual PE concentrations using UV-visible spectrophotometer. The quantity of the pendamethalin adsorbed from the solution was calculated using equation (3) presented earlier [18].

#### iii. Effect of adsorbent dosage

The adsorption of PE onto CBGNS was studied by changing the quantities of the adsorbents from 0.2g to 1.2g in the test solution while keeping the initial PE concentration at 60 mg/L, temperature = 25◦C,

pH 5 and equilibrium time 2hr. The mixtures were agitated with an orbital incubator shaker (Innova 4000 Model). At the completion of the contact, the solutions were filtered and the filtrate was analyzed for PE using uv-visible spectrophotometer [18].The quantity adsorbed was calculated from equation (1)

**iv. Effect of PE concentration**

To establish adsorption isotherms and the effect of pendamethalin concentration, aqueous solutions of PE were prepared, in a concentration range from 10 to 60 mg/L while keeping all parameters at optimized conditions and initial pendamethalin concentrations. Once the equilibrium has been attained, the quantity of adsorbed PE, as well as the residual concentration in solution, were determined. The mixtures were filtered. The unabsorbed PE in the filtrate was analyzed by UV-visible spectrophotometer [18]. The quantity of pendamethalin adsorbed, qe, was calculated using equation (1).

### 2.9.2. Adsorption Isotherm

Langmuir, Freundlich, Temkin and Dubinin-Radushkevich isotherm models were employed to describe the experimental results of effect of pendimethalin herbicide adsorption:

**i. Langmuir isotherm**

This describes quantitatively the formation of a monolayer adsorbate on the outer surface of the adsorbent, and after that no further adsorption takes place. Thereby, the Langmuir represents the equilibrium distribution of herbicide ions between the solid and liquid phases [19]. The Langmuir isotherm is valid for monolayer adsorption onto a surface containing a finite number of identical sites. It is an empirical isotherm model derived from a proposed kinetic mechanism, and it is based on four hypotheses: (a) the surface of the adsorbent is uniform, that is, all the adsorption sites are equal. (b) Adsorbed contaminant molecules do not interact. (c) All adsorption occurs through the same mechanism. (d) At the maximum adsorption, there is only a monolayer formed: Molecules of adsorbate do not deposit on other molecules of pollutant. Based upon these assumptions, Langmuir represented the following equation:

$$q_e = \frac{Q_{OK_l C_e}}{1+K_l C_e} \quad (5)$$

Langmuir adsorption parameters were determined by transforming the Langmuir equation (5) into linear form.

$$\frac{1}{q_e} = \frac{1}{Q_o} + \frac{1}{Q_{oKLC_e}} \quad (6)$$

Where:

$C_e$ = the equilibrium concentration of adsorbate (mg/L)

$q_e$ = the amount of herbicide adsorbed per gram of the adsorbent at equilibrium (mg/g).

$Q_o$ = maximum monolayer coverage capacity (mg/g)

$K_L$ = Langmuir isotherm constant (L/mg).

The values of $q_{max}$ and $K_L$ were computed from the slope and intercept of the Langmuir plot of $\frac{1}{qe}$ versus $\frac{1}{Ce}$[20]. The essential features of the Langmuir isotherm may be expressed in terms of equilibrium parameter RL, which is a dimensionless constant referred to as separation factor or equilibrium parameter [21]

$$R_{L=}\frac{1}{1+(1+K_{LC_O})} \quad (7)$$

Where:

$C_o$ = initial concentration

$K_L$ = the constant related to the energy of adsorption (Langmuir Constant).

$R_L$ value indicates the adsorption nature to be either unfavorable if $R_L$>1), linear if $R_L$ =1, favorable if 0< $R_L$<1 and irreversible if $R_L$=0.

### ii. Freundlich Adsorption Isotherm

This is commonly used to describe the adsorption characteristics for the heterogeneous surface [22]. These data often fit the empirical equation proposed by Freundlich:

$$Q_e = K_f C_e^{1/n} \quad (8)$$

Where $K_f$ = Freundlich isotherm constant (mg/g)

n = adsorption intensity

$C_e$ = the equilibrium concentration of adsorbate (mg/L)

$Q_e$ = the amount of metal adsorbed per gram of the adsorbent at equilibrium (mg/g). Linearizing equation (9), we have:

$$\text{Log}Q_e = logkf + \frac{1}{n} logC_e \quad (9)$$

The constant $K_f$ is an approximate indicator of adsorption capacity, while 1/n is a function of the strength of adsorption in the adsorption process [23]. If n = 1 then the partition between the two phases are independent of the concentration. If value of 1/n is below one it indicates a normal adsorption. On the other hand, 1/n being above one indicates cooperative adsorption [24]. The function has an asymptotic maximum as pressure increases without bound. As the temperature increases, the constants k and n change to reflect the empirical observation that the quantity adsorbed rises more slowly and higher pressures are required to saturate the surface. However, K*f* and *n* are parameters characteristic of the adsorbent-adsorbate system, which must be determined by data fitting and whereas linear regression is

generally used to determine the parameters of kinetic and isotherm models [25] Specifically, the linear least-squares method and the linearly transformed equations have been widely applied to correlate sorption data where 1/n is a heterogeneity parameter, the smaller 1/n, the greater the expected heterogeneity. This expression reduces to a linear adsorption isotherm when 1/n = 1. If n lies between one and ten, this indicates a favorable sorption process [26].

### iii. Temkin Isotherm

This isotherm contains a factor that explicitly taking into the account of adsorbent–adsorbate interactions. By ignoring the extremely low and large value of concentrations, the model assumes that heat of adsorption (function of temperature) of all molecules in the layer would decrease linearly rather than logarithmic with coverage [27]. As implied in the equation, its derivation is characterized by a uniform distribution of binding energies (up to some maximum binding energy) was carried out by plotting the quantity adsorbed $q_e$ against $lnC_e$ and the constants were determined from the slope and intercept. The model is given by the following equation [27].

$$q_e=\frac{RT}{b}\ln(A_{TC_e})$$

$$q_e = \frac{RT}{b_T}\ln A_{T+}(\frac{RT}{b})\ln C_e$$

$$B=\frac{RT}{bT}$$

$$q_e = B\ln A_T+B\ln C_e \quad (10)$$

Were;

$A_T$ =Temkin isotherm equilibrium binding constant (L/g)

$b_T$ = Temkin isotherm constant

R= universal gas constant (8.314J/mol/K)

T= Temperature at 298K.

B = Constant related to heat of adsorption (J/mol)

### iv. Dubinin–Radushkevich Isotherm Model

Dubinin–Radushkevich isotherm is generally applied to express the adsorption mechanism with a Gaussian energy distribution onto a heterogeneous surface [28, 29]. The model has often successfully fitted high solute activities and the intermediate range of concentrations data well

$$q_e= (q_s) \exp (-k_{ad\varepsilon^2} \quad (11)$$

$$Lnq_{e=} \ln (q_s)-( k_{ad\varepsilon^2}) \quad (12)$$

Where $q_e$, $q_e$, $K_{ad}$ , ε are $q_e$ = amount of adsorbate in the adsorbent at equilibrium (mg/g)

$q_s$ = theoretical isotherm saturation capacity (mg/g), $K_{ad}$ = Dubinin–Radushkevich isotherm constant ($mol^2/kJ^2$), ε = Dubinin–Radushkevich isotherm constant.

The approach was usually applied to distinguish the physical and chemical adsorption of herbicides molecule with its mean free energy, E per molecule of adsorbate (for removing a molecule from its location in the adsorption space to the infinity) can be computed by the relationship [30].

$$E = b\left[\frac{1}{\sqrt{2B_{DR}}}\right] \quad (13)$$

Where; $B_{DR}$ is denoted as the isotherm constant. Meanwhile, the parameter can be calculated as:

$$\varepsilon = RTln\left[1 + \frac{1}{c_e}\right] \quad (14)$$

Where;

R, T and $C_e$ represent the gas constant (8.314 J/mol K), absolute temperature (K) and adsorbate equilibrium concentration (mg/L), respectively. One of the unique features of the Dubinin-Radushkevich (DRK) isotherm model lies on the fact that it is temperature-dependent, which when adsorption data at different temperatures are plotted as a function of logarithm of amount adsorbed vs. the square of potential energy, all suitable data will lie on the same curve, named as the characteristic curve [31]. The equation (11) is linearized to equation (12) which is used in the plot of DRK model.

### 2.9.3. Kinetic studies

The study of adsorption kinetic of pendimethalin onto the carbonized banbara groundnut shell describes the solute uptake rate and evidently this rate controls the residence time of adsorbate uptake at the solid-solution interface. Effects of adsorption kinetics on PE were studied by varying the contact time as 5, 10, 15, 20, 30, 40, 50, 60, 80, 100 and 120min. by keeping all other parameters (pH=5, adsorbent dosage 0.2g, initial PE concentration= 60mg/l, T= 298K) at optimized values. The rate constants of the adsorption process were determined from the pseudo – first -order and pseudo-second-order equations. For the pseudo-first-order kinetics, the linear Lagergren [32] expression given equation (15) was used:

$$\log (q_e - q_t) = \log(q_e) - \frac{K_1}{2.303}t \quad (15)$$

Where $k_1$ is the first-order rate constant and *q*e and *qt* are the amounts of PE adsorbed at equilibrium and time *t* (mg/g), respectively. The values of log *(q*e − *qt )* were calculated from the experimental data and plotted against *t*. $k_1$was calculated from the slope of the plot. The linear form of the pseudo-second-order reaction kinetic model [31] also used for adsorption studies can be given by equation (16)

$$\frac{t}{q_t} = \frac{1}{K_2 q_e^2} + \frac{1}{q_e}\ (t) \quad (16)$$

Where the equilibrium adsorption capacity (qe), and the second order constant $k_2$ (g/mg h) can be determined experimentally from the slope and intercept of plot t/qt versus t. The Elovich kinetic model was described in literature by many authors according to the following linear relation in equ. (17) [33]:

$q$t= 1/$\beta$ ln($\alpha\beta$) + (1/$\beta$) ln$t$ (17)

The parameters ($\alpha$) and ($\beta$) can be calculated from the slope and intercept of the linear plot of $q$t versus ln(t). The third kinetic model used is the intra particle diffusion and is described by equation (18) [34]:

$q$e= $C$ + $k_{int}^{1/2}$ (18)

The constant $k_{int}$ (mg /g $min^{0.5}$) is the intra particle diffusion rate and $C$ is the boundary layer thickness.

### 2.8. Thermodynamic parameters

The temperature of the working solution was varied between 30 to 60 °C (30, 40, 50 and 60 °C). 10$cm^3$ of the optimum concentration, 60 mg/L PE, was contacted with 0.2g of CBGNS for 80 min in 100$cm^3$ conical flasks. The mixtures were equilibrated at contact time at aforementioned temperatures. The mixtures were filtered, and the filtrates were analyzed for PE using UV-visible spectrophotometer, and the quantities adsorbed were calculated by using Eq. (3) [35]. The thermodynamic parameters such as changes in free energy (ΔG), enthalpy (ΔH) and entropy (ΔS) give useful view about the feasibility and the spontaneous nature of the adsorption process and generally can be described thus (19, 20 and 21) : .

$\Delta G = -RT\ln k_c$ (19)

$\ln k_c = -\Delta G/RT = -(\Delta H/RT) + (\Delta S/R)$ (20)

Where $R$ is the gas constant (8.314 J/molK), $T$ is the absolute temperature ($K$), and $k_c$ is the thermodynamic equilibrium constant and can be obtained from the relation as in equation (21) [36]:

$k_c = C_a/C_e$ (21)

Where $C_a$ is mg of PE adsorbed per liter and $C_e$ is the equilibrium PE concentration of solution (mg/L). Both ΔHand ΔG can be obtained from the slope and the intercept of van't Hoff plot of ln$K_c$ versus 1/$T$

## 3. Results and discussion

### 3.1. FT-IR spectroscopy and scanning electron spectroscopy

The FTIR spectra of CBGNS before and after adsorption on pendimethalin are given in figure (1a-b). The broad band at 3391$cm^{-1}$ is attributed to the stretching vibration of -OH group. The stretching of the -OH group bond to methyl radicals is attributed to the signal at 2877$cm^{-1}$. Also, peaks at 2344$cm^{-1}$ and 2110$cm^{-1}$ are associated with the stretched vibration of alkynes C≡C, while the peak at 1994$cm^{-1}$ is

ascribed to be C=O group which is affected by minor overlapping with C-C aromatic ring stretched vibrations. The broad peak at 1033cm$^{-1}$ is associated to C-O group which confirms the lignin structure of CBNS. The peaks at 1562cm$^{-1}$ and 1402cm$^{-1}$ are associated with stretching vibrations of aromatic and C-H in alkane, while the peak at 747cm$^{-1}$ and 870cm$^{-1}$ are due to stretched vibration of C-O in aromatic, esters and ethers. Figure 1b shows FTIR spectra of CBGNS after adsorption. There was a shift and broadening of adsorption peaks after adsorption. The shift of the -OH peak from 3391cm$^{-1}$ to 3152cm$^{-1}$ shows the engagement of the -OH group in adsorption. The shift of the carbonyl group peak from 1033cm$^{-1}$ to 1030cm$^{-1}$ shows that carbonyl group participated in the adsorption of PE. The presence of these functional groups and their enhancement in adsorption abilities of CBGNS agrees with the findings of [37].

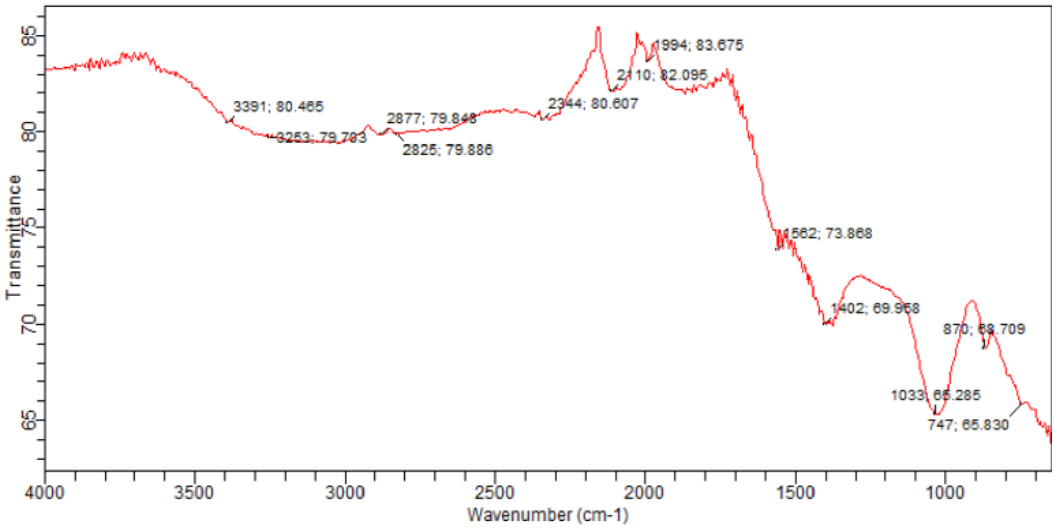


**(a)**

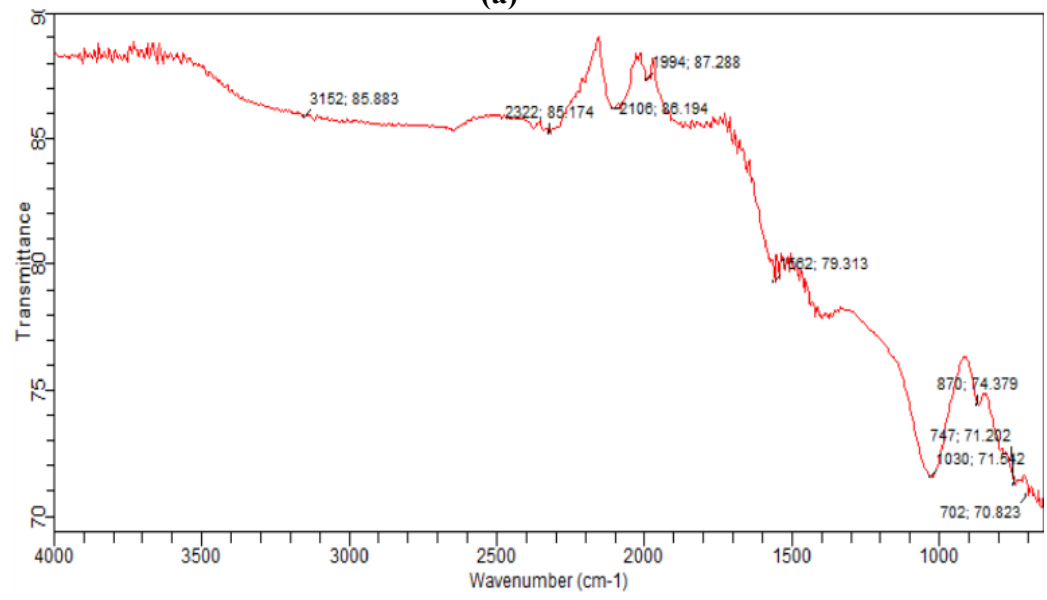


**(b)**

**Figure (1a-b)** FTIR Spectrum of CBGNS before and after adsorption on Pendimethalin

The SEM micrograph of the CBGNS before and after adsorption on PE is shown in (figure 2a-b) Results showed that the surface structure of CBGNS before and after adsorption on PE obtained are different from each other. The surface is smoother after adsorption. Probably, due to the deposition of PE by physical adsorption or progressive change in CBGNS.

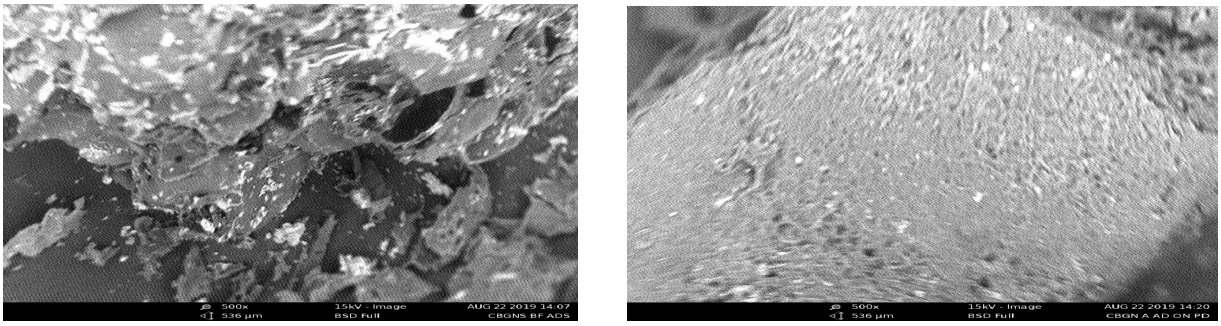

**(a)** **(b)**

**Figure (2a-b)** SEM Micrographs of CBGNS before and after adsorption on PE

### 3.2. Physical Properties of the Produced Carbonized Carbon

Some physical properties of the carbonized carbon produced are given in the Table 1. The value of the moisture content, pore volume and the bulk density of the produced carbonized carbon revealed that it had good adsorptive properties. It was noticed from the properties of the carbonized carbon that, though it might not give up to 100% adsorption, it will be good for adsorption of organic substances to a very large extent [38].

**Table 1.** Physical property of the CBGNS

| Method | Moisture content | Density | Pore volume |
|---|---|---|---|
| CBGNS | 16.8% | 0.199g/cm$^3$ | 1.89cm |

### 3.3. Optimized adsorption parameters

The removal of PE from the aqueous solution is strongly affected by the pH of the solution as illustrated in Fig. 1. The PE removal were somewhat evidently dependent on pH with the better adsorption occurring under acidic conditions (pH 6). Therefore, the removal of PE at higher pH values greater than 6 was due to the formation of precipitates rather than adsorption [39]. The increase in adsorption with an increase in pH is due to a decrease in competition between hydrogen ions and PE molecules for the surface sites and also due to a decrease in positive surface charge. As the pH increases, more negatively charged surface becomes available and thus facilitates greater PE adsorption [40].

The effect of adsorbent dosage on the adsorption of PE onto CBGNS was studied by varying amounts of adsorbent dosage from (0.2 to 1.2g) while other parameters were kept constant. Fig.2 revealed that

the amount of PE adsorbed first increased with an increase in adsorbent dosage due to increased surface area and more adsorption sites available for binding of PE [5]. Maximum removal was attained at 0.2g. After 0.2g of adsorbent dosage there was no significant change in the amount of PE removed. The decrease in adsorption per unit mass with increasing dosage of adsorbent is attributed to possible overlapping of adsorption sites as adsorbent dosage increases which will equally reduce the effective adsorption sites. It was observed that as the adsorbent dosage decreased from 0.2 to 1.2g. The quantity adsorbed (mg/g) decreased from 2.256 to 0.302mg/g.

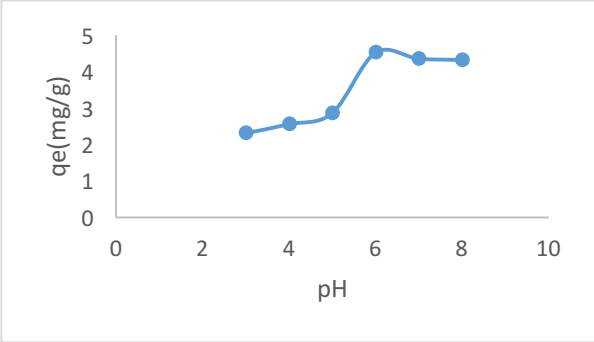


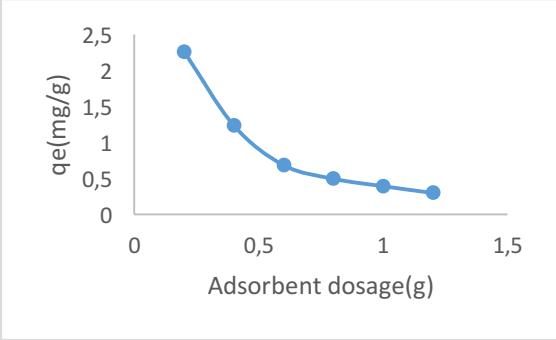


**Figure 1.** Effect of pH on adsorption of PE onto CBGNS. **Figure 2.** Effect of dosage on adsorption

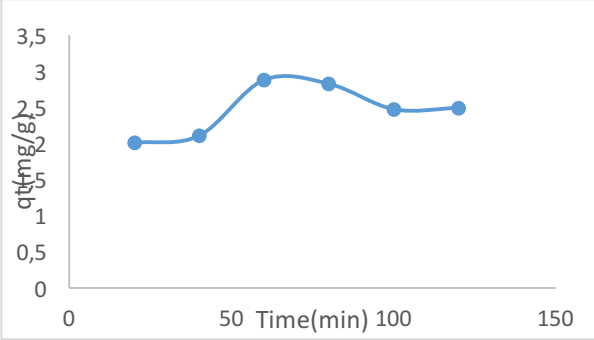


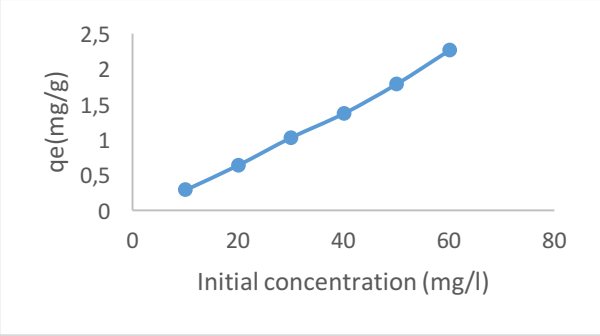


**Figure 3.** Effect of time on adsorption of PE onto CBGNS.

**Figure 4.** Effect of initial concentration on adsorption of PE onto CBGNS.

The effect of contact time on adsorption efficiency of PE onto CBGNS was assessed by varying the contact time from 20 – 120 min with other parameters kept constant as given in Fig. 3. From the plot, it is evident that the rate increased quickly with time, and then reached equilibrium. The adsorption capacity and percent removal of PE onto the adsorbent significantly increased during the initial adsorption stage, and then equilibrium was nearly reached. Hence, in the present work, 60 min was chosen as the equilibrium time. Generally, the removal rate of adsorbate is rapid initially, but it gradually decreases with time until it reaches equilibrium. This can be explained due to the fact that a large number of vacant surface sites are available for adsorption at the initial stage, and after a lapse of time, the remaining vacant surface sites are not easy to be occupied due to repulsive forces between the solute molecules on the solid and bulk phases [41].

The effect of initial PE concentration was investigated by varying the concentration from 10 to 60mg/L. Fig. 4 shows plots for the variation of the equilibrium amount of PE adsorbed. It is evident from the plots that the amounts of PE adsorbed by CBGNS increases with increasing concentration. At low concentration, the available driving force for transfer of PE molecules onto the adsorbent particle is low. While at high concentration, there is a corresponding increase in the driving force, thereby, enhancing the interaction between the PE molecules in the aqueous phase and the active sites of the adsorbent. As a result of this, there was an increase in PE uptake.

### 3.4. Adsorption Isotherm

Adsorption isotherm studies were carried out using four isotherm models: The Langmuir, Freundlich, Temkin and Dubinin-Radushkevich isotherm models. The linear plot of specific adsorption (1/qe) against the equilibrium concentration (1/Ce) for Langmuir model, (logqe) against the (logCe) for Freundlich model, (lnCe) against the equilibrium adsorption (qe) for Temkin model and (lnqe) against $\varepsilon^2$ for Dubinin-Radushkevich model (Figure not shown)

The adsorption of PE using CBGNS were well described by Freundlich followed by Langmuir isotherm model. This revealed that the adsorption process was governed by monolayer, and at same time heterogeneous adsorption.

From the data calculated in table 2. The $R_L$ value for PE adsorption is greater than 0 but less than 1 indicating that the Langmuir isotherm is favourable. The values of 'n' from Freundlich model (Table 2) ranged 1 – 10 which suggests that the adsorption process for PE adsorption onto CBGNS is favourable. The values of 'n' are greater than 1 indicating molecular interaction between CBGNS and the PE molecule. These results are in agreement with that of Li *et al*. [42].

**Table 2**. Langmuir, Freundlich, Temkin and Dubinin–Radushkevich Isotherm constants for the adsorption of PE molecule onto CBGNS

| Herbicide | Langmuir | | | | Freundlich | | | |
|---|---|---|---|---|---|---|---|---|
| PE | $Q_o$(mg/g) | $K_L$(L/mg) | $R_L$ | $R^2$ | 1/n | N | $K_f$ | $R^2$ |
| | 23.81 | 0.045 | 0.212 | 0.990 | 0.657 | 1.523 | 0.617 | 0.994 |
| | Temkin | | | | Dubinin-Raduskevich | | | |
| | $A_T$(L/mg) | B | $b_T$ | $R^2$ | $q_s$(mg/g) | $K_{ad}$(mol$^2$/KJ$^2$) | E(KJ/MoL) | $R^2$ |
| | 0.243 | 28.89 | 85.73 | 0.867 | 31.31 | $6x10^{-6}$ | 0.289 | 0.621 |

From the Temkin plot not shown, the following values were estimated: $A_T$ = 0.243 L/g, B=28.89J/mol for PE molecule which is an indication of the heat of adsorption indicating a physical adsorption process and the $R^2$ value of 0.867. From the linear plot of DRK model, qs was determined to 31.31mg/g, the

mean free energy, E= 0.287KJ/mol indicating a physisorption process and the $R^2$= 0.621. Comparing the values of the correlation coefficient, $R^2$, for the four tested isotherms, it can be observed that the adsorption data of PE onto CBGNS fitted well with the Freundlich isotherm, followed by Langmuir isotherm followed by Temkin and the least is Dubinin–Radushkevich isotherm.

### 3.5. Adsorption Kinetics

The mechanism and the rate determining step of an adsorption reaction can be determined by modeling into kinetic models. The pseudo-first order, pseudo-second order and Elovich models were used to determine the rate constants for adsorption of CBGNS onto PE molecule. An intra -particle diffusion model was also applied to get some hints about the mechanism of reaction. As can be seen in table 3 the pseudo- first-order equation did not fit well to the whole range of contact times. The experimental qe values do not agree with the calculated qt from the linear plots. This shows that the adsorption of PE onto CBGNS did not follow first-order kinetic indicating that the adsorption was not diffusion-controlled and adsorption was not preceded by diffusion through a boundary [43]. The pseudo-second-order kinetic model fits the experimental data quite well; the correlation coefficients values, $R^2$, all up to unity, and the experimental and theoretical uptakes are in good agreement. This indicates the applicability of the second-order kinetic model to describe the adsorption process of PE onto CBGNS. Elovich model gives useful information on the extent of both surface activity and activation energy for chemisorption process. The Elovich plots does not fit kinetic data. The plot of qt against $t^{½}$ is not linear (figure not shown), indicating that the adsorption process of PE and onto CBGNS involves more than one step. In the first step, the mass transfer of the adsorbate to the external surface of the adsorbent takes place. The intra particle transport of adsorbate in the adsorbent pores occurs in the second step. The values of $R^2$ for the three initial concentrations found when the intra particle diffusion model is applied are lower than those for the pseudo-second-order model (Table 4), which is further evidence supporting a better correlation between pseudo-second-order model and the experimental data.

**Table 3.** Kinetic models for the adsorption of CBGNS onto PE molecule

| **Kinetic Model** | **Parameters** | | | |
|---|---|---|---|---|
| **Pseudo-first order** | $q_{eExp}$(mg/g)<br>14.64 | $q_{eCal}$(mg/g)<br>0.955 | $K_1$($min^{-s}$)<br>0.016 | $R^2$<br>0.900 |
| **Pseudo-second order** | $q_{eExp}$(mg/g)<br>14.64 | $q_{eCal}$(mg/g)<br>14.71 | $K_2$($min^{-s}$)<br>0.079 | $R^2$<br>0.999 |
| **Elovich** | | B<br>3.067 | A<br>$6.9 \times 10^{16}$ | $R^2$<br>0.914 |
| **Intra-particle diffusion** | | $K_3$<br>0.113 | C<br>13.43 | $R^2$<br>0.880 |

**Table 4. Comparison of Pendimethalin Langmuir adsorption capacity onto carbonized Bambara groundnut shell with different order adsorbents**

| Adsorbate | Adsorbent | Adsorption capacity $q_e$(mg/g) | Lit. References |
|---|---|---|---|
| Atrazine | Desert date seed shell | 0.780 | [44] |
| Paraquat dichloride | Bambara groundnut shell | 83.33 | [2] |
| Copper ions | Fish scales derived biochar | 39.39 | [45] |
| Atrazine | Bambara groundnut shell | 3.52 | [6] |
| Cadmium | Water melon rind | 53.48 | [46] |
| Zinc (II) | magnetite | 52.63 | [37] |
| Carbenazim | Spent coffee grounds | 11.92 | [47] |
| Pendimethalin | Bambara groundnut shell | 23.81 | This study |

### 3.6. Thermodynamic studies

The studies of temperature influence on herbicide adsorption available in the literature reveal that the relation between temperature and adsorption depends on the adsorbent/adsorbate pair [48]. In order to study the nature of adsorption, the thermodynamic parameters for the adsorption process, such as the Gibbs free energy (ΔG), the enthalpy (ΔH) and the entropy (ΔS) were calculated using Equations (14) and (15). The values of ΔH and ΔS were calculated from the slope and intercept of plot between lnKc versus 1/T are shown in Table 5. The positive value of ΔH indicated the endothermic nature of the adsorption interaction. The positive value of ΔS imply an increase in randomness of the solid – adsorbate interphase in the solution. The negative value of ΔG indicated the feasibility of the process and the spontaneous nature of the adsorption with a high preference of pendimethalin on the surface of the studied adsorbent. ΔG values were found to decrease as the temperature increased, indicating higher driving force and hence resulting in more adsorption capacity. Similar result was reported elsewhere by other authors [49].

Table 5: Thermodynamic parameters for the adsorption of PE onto CBNS

| T(K) | ΔG(KJ/mol) | ΔH(KJ/mol) | ΔS(J/mol.K) |
|---|---|---|---|
| 303 | -6.854 | 15.77 | 56.30 |
| 313 | -6.464 | | |
| 323 | -3.949 | | |
| 333 | -3.269 | | |

## Conclusion

The carbonized carbon prepared from Bambara groundnut shells was successfully used for the removal of pendimethalin herbicide from aqueous solutions and can therefore be considered as a promising adsorbent for waste water treatment. Adsorption of pendimethalin herbicide was highly pH dependent and the results showed that the optimum pH for the removal of PE was found to be 6, where PE exist mostly as the most easily adsorbed form. PE concentration increases as the initial concentration was increase and the contact time for total PE removal was obtained at 60 mins. Adsorption equilibrium data were fitted to Langmuir, Freundlich, Temkin and Dubinin-Radushkevich isotherm models and the equilibrium data for CBGNS were best represented by the Freundlich isotherm. The adsorption kinetics was found to fit well to pseudo second-order kinetic model. Thermodynamic parameters such as enthalpy (ΔH), entropy (ΔS) and free energy (ΔG) were evaluated.

## Conflict of Interest

The authors declare that the research was conducted in the absence of any commercial or financial relationships that could be construed as a potential conflict of interest.

## References

[1] G. M. Zuhra, M. I. Bhanger, A. Mubeena, N. T. Farah, R. M. Jamil, Adsorption of methyl parathion pesticide from water using watermelon peels as a low cost adsorbent. Chemical Engineering Journal 138, 616–621 (2008).

[2] A. M. Ayuba and T. A. Nyijime, Paraquat dichloride adsorption from aqueous solution using carbonized Bambara groundnut shells. *Bayero Journal of Pure and Applied Sciences*, 12, 1:167 – 177 (2019)

[3] S. Neera, Adsorption of herbicides on coal fly ash from aqueous solutions, *Journal of Hazardous Materials,* 168: 233–237 (2009).

[4] C. R. Worthing, Farnham, British Crop Protection Council. *The pesticide manual*, 9th ed. (1991).

[5] A. M Ayuba and T**.** A Nyijime**,** Removal of Pendimethalin Herbicide from Aqueous Solution Using Untreated Bambara Groundnut Hulls as a Low-Cost Adsorbent, *J. Mater. Environ. Sci*., 12, 1: 15-26 (2021).

[6] E. Sebata, M. Moyo, U. Guyo, N.P. Ngano, B.C. Nyamunda, F. Chigondo, M.S. Chitsa, Adsorptive Removal of Atrazine from Aqueous Solution Using Bambara Groundnut Hulls. *International Journal of Engineering Research & Technology*, 2, 5: 312 – 321 (2013).

[7] T. Nharingo, N. M. Muzondo, E. Madungwe, F. Chigondo, U. Guyo, B. Nyamunda, Isotherm Study of the Biosorption of Cu (II) from Aqueous Solution by *Vigna subterranean* (L.)Verdc Hull. *International Journal of Scientific and Technology Research*, 2, 4: 199 – 206 (2013).

[8] L. K. Akinola, A. Ibrahim, A. S. Chadi, Kinetic and Equilibrium Studies of Congo Red Adsorption on Adsorbent from Bambara Groundnut Hulls Al-Hikmah, *Journal of Pure & Applied Sciences,* 2, 2: 79-88 (2013).

[9] V. A. Jideani, C. F. Diedericks, Nutritional, Therapeutic, and Prophylactic Properties of *Vig na subterranea* and *Moringa oleifera*. In: Antioxidant-Antidiabetic Agents and Human Health, Janeza Trade line 9, 51000 Rijeka, Croatia, P187 – 201 (2014).

[10] L. Mahardiani, A. Ashadi, S. Saputro, N. Y. Indriyanti, M. Taufiq, The Removal of Organic Pollutant from Aqueous Solution by Modified Activated Carbon Surface. *Mor. J. Chem.* 8, 4: 936-942 (2020).

[11] C. Ash, B. Satapathy, D. Mukherjee, P.S. Nanda, B. Gumaste, J. L. Mishra, Characterization and application of activated carbon prepared from coir pith, *J. Sci. Ind. Res*. 65, 1008-1012 (2006).

[12] ASTM, Standards, ASTM International, West Conshohocken, Method D6751-08; Alcoholysis for Biodiesel Fuel Production and Application of the Reaction to Oil Processing. *Journal of Molecular Catalysis B: Enzymatic*, 76, 133-142.

[13] AOAC Official Methods of Analysis, AOAC International Washington D.C 17th Edn, pp. 1456-1500 (2005).

[14] G. I. Onwuka, Food Analysis and Instrumentation*: Theory and Practice*. 2nd Ed. Naphtali Prints, Lagos, 179-228 (2018).

[15] A. M. Ayuba and B. Idoko, Kinetic, equilibrium and thermodynamic studies on the adsorption of Crystal Violet dye from Aqueous Solution using Activated Cowpea (*Vigna Unguiculata)* Husk, Applied *Journal of Environmental Engineering Sciences,* 6, 2: 182-195 (2020).

[16] A. A. Abia, and E. D. Asuquo, Lead (II) and Nickel (I) adsorption kinetics from aqueous metal solutions using chemically modified and unmodified agricultural adsorbents. *Afr J Biotechnol,* 5, 16: 1475–1482 (2006).

[17] O. Saidat, J. S. Giwa, A. A. Moses, A. Adeyi, and G. Abdulwahab, Adsorption of Atrazine from AqueousSolution Using Desert Date Seed Shell Activated Carbon. *ABUAD Journal of Engineering Research and Development*, 1, 3: 317-325 (2018).

[18] F. A. Adekola, N. Abdus-Salam, L. B. Abdul-Rauf, Removal of arsenic from aqueous solution by synthetic hematite. *J Chem Soc Niger,* 36, 2:52–58 (2011).

[19] T. H. Vermeulan, K. R. Vermeulan, L. C. Hall, Fundamental‘‘*Ind. Eng. Chem.* 212–223 (1966).

[20] I. Langmuir, The adsorption of gases on plane surfaces of glass, mica and platinum, *J. Am. Chem. Soc*. 40: 1362-1403 (1918).

[21]T. N. Webber, R. K. Chakravarti, Pore and Solid Diffusion Models for fixed bed adsorbers. *J.Am.Inst.Chem.Eng*. 20: 228-238 (1974).

[22] N. D. Hutson, R. T. Yang, Synthesis and characterization of the sorption properties of oxygen-binding cobalt complexs immobilized in nano porous material. *Industrial and engineering chemistry research*. 39: 2252-2259, (2000).

[23] E. Voudrias, F. Fytianos, E. S. Bozani, E.S. (2002). Sorption Description isotherms of Dyes from aqueous solutions and Waste Waters with Different Sorbent materials, *Global Nest, The Int. J.* 4, 1: 75-83 (2002).

[24] S. Mohan, J. Karthikeyan, Removal of lignin and tannin color from aqueous solution by adsorption on to activated carbon solution by adsorption on to activated charcoal, *Environ. Pollution.* 183-187 (1997).

[25] R. Guadalupe, H. E. Reynel-Avila, A. Bonilla-Petriciolet, I. Cano-Rodríguez, C. Velasco-Santos, A. L. Martínez-Hernández, Recycling poultry feathers for Pb removal from wastewater: kinetic and equilibrium studies, *Proceedings of World Academy of Science, Engineering and Technology,* 30 (2008)

[26] S. Goldberg, Equations and Models Describing Adsorption Processes in Soils‘‘. *Soil Science Society of America*, 677 S. Segoe Road, Madison, WI 53711, USA. *Chemical Processes in Soils. SSSA* Book, 8 (2005).

[27] C. Aharoni, M. Ungarish, kinetic of activated chemisorption: Theoretical models, *J. Chem. Soc. Faraday Trans*. 73: 456–464 (1977).

[28] A. Gunay, E. Arslankaya, I. Tosun, Lead removal from aqueous solution by natural and pretreated clinoptilolite: adsorption equilibrium and kinetics, *J. Hazard. Mater*. 146: 362–371 (2007).

[29] A. Dabrowski, adsorption—from theory to practice, *Adv. Colloid Interface Sci*.93, 135–224. Department of Chemical Technology Midlands State University Gweru, Zimbabwe. *International Journal of Engineering Research &Technology*, 2, 5: 2278-0181 (2001).

[30] M. M. Dubinin, The potential theory of adsorption of gases and vapors for adsorbents with energetically non-uniform surface, *Chem. Rev*, 60 235–266 (1960).

[31] K. Y. Foo, B. H. Hameed, Insights into the modeling of adsorption isotherm systems, *Review Chemical Engineering Journal*, 156, 2–10 (2010).

[32] G. O. Achieng, V. O. Shikuku, Adsorption of copper ions from water onto fish scales derived biochar: Isothermal perspectives. *J. Mater. Environ. Sci.,* 11: 1816-1827 (2020).

[33] N. Hassan, A. Shahat, A. El-Didamony, M.G. El-Desouky, A.A. El-Bindary, Equilibrium, Kinetic and Thermodynamic studies of adsorption of cationic dyes from aqueous solution using ZIF-8. *Mor. J. Chem.* 8, 3: 627-637 (2020).

[34] I. A. Nnanwube, O. D. Onukwuli, V. N. Okafor, J. I. Obibuenyi, R. O. Ajemba, C. C. Chukwuka, Equilibrium, Kinetics and Optimization Studies on the Bleaching of Palm Oil Using Activated Karaworo Kaolinite. *J. Mater. Environ. Sci.,* 11: 1599-1615 (2020).

[35] A. M. Ayuba and T. A. Nyijime, Kinetic and equilibrium studies of paraquat dichloride adsorption on raw Bambara groundnut (*Vigna subteranean*) shells, *Appl. J. Envir. Eng*. Sci. 6, 1: 1-13 (2020).

[36] A. D. N'diaye, M. Sid'A. Kankou, Sorption of caffeine onto low-cost sorbent: Application of two and three-parameter isotherm models. *Appl. J. Envir. Eng. Sci.* 5, 3: 263-272 (2019).

[37] N. Abdus-Salam, and S. K. Adekola, Adsorption studies of zinc (II) on magnetite, baobab (*Adansonia digitata*) and magnetite–baobab composite *Applied Water Science*, 28-222 (2018). https://doi.org/10.1007/s13201-018-0867-7

[38] P. Sugumaran, V. S. Priya, P. Ravichandran, and S. Seshadri, Production and Characterization of Activated Carbon from Banana Empty Fruit Bunch and *Delonix regia* Fruit Pod, *Journal of Sustainable Energy & Environment* 3: 125-132 (2012).

[39] D. Prahas, Y. Kartika, N. Indraswati, and S. Ismadji, Activated carbon from jackfruit peel waste by $H_3PO_4$ chemical activation: pore structure and surface chemistry characterization, *Chemical Engineering Journal*, 140: 32–42 (2008).

[40] B. Bayat, Comparative study of adsorption properties of Turkish fly ashes 1. The case of nickel (II), copper (II) and zinc (II). *Journal of Hazard Material,* 144:251–273 (2002).

[41] Y. B. Onundi, A. A. Mamun, M. F. Al Khatib, Y. M. Ahmed, Adsorption of copper, nickel and lead ions from synthetic semiconductor industrial wastewater by palm shell activated carbon. *International Journal of Environmental Science Technology* 7:751–758 (2010).

[42] F. A. Ugbe and N. Abdus-Salam, Kinetics and thermodynamic modelling of natural and synthetic goethite for dyes scavenging from aqueous systems, *Arabian Journal of Chemical and Environmental Research*, 7, 12–28 (2020)

[43] S. Sener, Use of solid wastes of the soda ash plant as an adsorbent for the removal of anionic dyes: Equilibrium and kinetic studies*, Chemical Engineering Journal,* 138: 207- 214 (2008).

[44] S. O. Giwa, J. S. Moses, A. A. Adeyi, A. Giwa, Adsorption of Atrazine from Aqueous Solution Using Desert Date Seed Shell Activated Carbon. *ABUAD Journal of Engineering Research and Development (AJERD)* 3: 317-325 (2018)

[45] G. O. Achieng, V. O. Shikuku, Adsorption of copper ions from water onto fish scales derived biochar: isothermal perspectives, *journal of materials and environmental science*, 11: 1816-1827 (2020)

[46] Z. D. Husein, E. Aazam, M. Battia, Adsorption of Cadmium (II) onto Watermelon Rind Under Microwave Radiation and Application into Surface Water from Jeddah, Saudi Arabia. *Arab J Sci Eng*. (2017).

[47] H. Ali, N. Mladenka, I. Mihajlović, Sorption of carbendazim and linuron from aqueous solutions with activated carbon produced from spent coffee grounds: Equilibrium, kinetic and thermodynamic approach, *Journal of Environmental Science and Health*, (2018).

[48] V. Arora, D. P. Tiwari, Analysis of adsorptive characteristics of chemically modified bio-waste walnut shell for degradation of brilliant yellow dye, *Appl. J. Envir. Eng. Sci*. 5, 3: 231-240 (2019).

[49] D. Ma, S. Zhang, S. Zhan, L. Feng, S. Zeng, Q. Lin, Y. Pan, Adsorptive Removal of Catechol from Aqueous Solution with a Water-Stable and Hydroxyl-Functionalized Terbium–Organic Framework, *Ind. Eng. Chem. Res.* 58, 43: 20090–20098 (2019).

---